CONSTITUTIVE MODELLING OF HIGH STRAIN-RATE DEFORMATION: APPLICATION TO ADIABATIC SHEAR BANDING

Y. ESTRIN[1] and A. MOLINARI[2]
[1]Department of Mechanical and Materials Engineering
The University of Western Australia, Nedlands WA 6907, Australia
[2]LPMM, Universite de Metz, Ile du Saulcy, F-57045 Metz, Cedex, France

ABSTRACT

One of the mechanisms of failure of metallic materials is adiabatic shear banding - localization of plastic strain caused and accentuated by softening associated with heat release during the deformation process. Constitutive models suitable for describing deformation at very high strain rates will be discussed. Particular emphasis will be put on the effect of the strain rate and temperature dependence of the strain hardening coefficient on the propensity of a material for adiabatic shear banding. The role of metallurgical variables, such as the spacing between second-phase particles will be discussed.

KEYWORDS

Adiabatic shear bands, constitutive modelling, strain localization, high-speed deformation, rate and temperature effects.

INTRODUCTION

An important mechanism of failure of structural materials under high rate of deformation is associated with strain localization in what is commonly referred to as adiabatic shear bands (Bai and Dodd, 1992). This term suggests that the effect is related to heat release during the deformation process and that the rate of heat removal is sufficiently small for the notion of adiabaticity to be of relevance. Localized deformation bands formed under these conditions tend to be preferred sites for damage accumulation that eventually leads to fracture. Engineering applications where this phenomenon is prevalent include high-speed forming and metalworking, crashworthiness in automotive and aerospace industries, armour penetration, and other impact dynamic problems. On a more microscopic scale, strain localizations may affect propagation of cracks in metallic materials, shearing of asperities in frictional sliding, etc. This is why deformation with high rate of strain, of the order of 10^3 s^{-1} and above, has been attracting the attention of engineers and researchers for decades. A considerable amount of experimental data on adiabatic shear banding in a broad range of materials has been accumulated to date (Bai and Dodd, 1992; Chiem et al., 1988; Meyers et al., 1992; Murr et al., 1995). A number of theoretical models aiming at describing high strain rate deformation in general and adiabatic shear banding in particular

are in existence (Armstrong and Zerilli, 1988; Bodner, 1988; Culver, 1973; Fressengeas and Molinari, 1987; Johnson and Cook, 1985; Molinari and Clifton, 1987). Most of these models are phenomenological in nature, and - despite their generally good descriptive capabilities - they give little guidance as to the design of materials with high resistance against adiabatic shear banding. Such guidance can be expected to be provided by microstructure-related constitutive models, notably those based on internal state variables associated with dislocation densities (Kocks, 1976; Estrin and Mecking, 1984; Klepaczko and Chiem, 1986; Follansbee and Kocks, 1988). In the present talk we shall give a brief review of the models currently in use and then focus on some new developments which emphasize the microstructural aspects of constitutive modelling. A model based on dislocation density evolution (Estrin and Mecking, 1984; Estrin, 1996; Estrin et al., 1996), which makes it possible to predict the effect of metallurgical structure on the propensity of a material to adiabatic shear banding, will be presented.

PHENOMENOLOGICAL MODELS AND STRAIN LOCALIZATION CRITERIA

Some Empirical Facts and Models

An adiabatic shear band is a result of strain localization leading to a higher local rate of heat release and the attendant local softening of the material which, in turn, accentuates plastic strain localization. This thermomechanical coupling comes to bearing for sufficiently high rates of plastic deformation and is facilitated in materials with poor thermal conductivity and low heat capacity, as illustrated by unstable deformation behaviour of metals at cryogenic temperatures (Molinari et al., 1993). Of course, the heat generation conditions in a localized deformation band are far from adiabatic, but historically this term has been used to emphasize the thermal nature of the shear bands. The idea of local softening due to heat release associated with plastic work goes back to early works by Farren and Taylor (1925) and Stepanov (1933) who put forward a hypothesis of local amorphization, or even melting, in the vicinity of slip planes. Though this would certainly represent an overestimation of the effect in most cases, evidence of thin solidified melt layers at the centre of shear bands was found (cf. Hartmann et al., 1981). Although the local heating effect is generally less dramatic than that, a temperature rise of several hundred degrees is quite common, and this may be sufficient for a phase transformation to occur, as is the case in steels and titanium alloys. This can result in the formation of *transformed shear bands*, which can be visualized most easily. In the literature, a distinction is made between such *transformed shear bands* and *deformed shear bands* which are simply localized zones of intense plastic shear which do not undergo a phase transformation. An example of a transformed shear band associated with a martensitic transformation in the localized deformation zone is presented in Fig. 1. A deformed band is shown in Fig. 2.

Obviously, adiabatic shear bands are the weaker parts of a structural component. Transformed bands are more brittle than the surrounding material and provide sites for brittle cracking, while deformed bands which underwent large strains are zones with increased damage and are prone to ductile failure. Generally, adiabatic shear bands can be considered as precursors to brittle or ductile fracture. (Bai and Dodd, 1992).

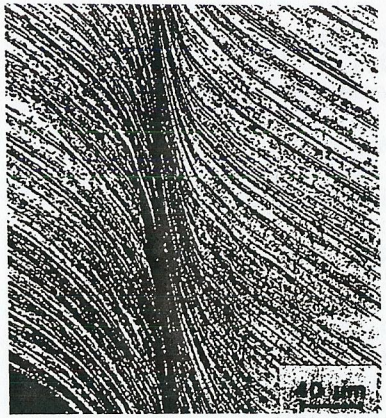

Fig. 1. Deformed shear band in a plate that underwent a high velocity impact (after Bai and Dodd 1992)

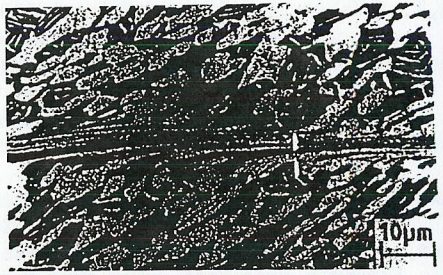

Fig.2. Transformed shear band in a titanium alloy (after Bai and Dodd 1992).

The phenomenology of adiabatic shear bands has been discussed extensively (cf. Bai and Dodd, 1992; Meyers et al., 1992, Murr et al., 1995). The salient features of adiabatic shear banding include a large local strain (5 to 100), a high shear strain rate (of the order of 10^4 -10^6 s^{-1}), and a high local temperature. They are usually non-crystallographic and have a thickness of tens to hundreds micrometers. No clear correlation of the band thickness with the grain size could be established which suggests that a characteristic length scale is determined by other factors, such as heat conduction and, possibly, other non-local effects. Often periodic patterns of adiabatic shear bands are found (Bai and Dodd, 1992; Nesterenko et al., 1995).

Although adiabatic shear banding plays a detrimental role in many engineering situations, there are cases where it is desirable. Examples can be found in metal cutting, where formation of adiabatic shear bands facilitates fragmentation of chips, or in armour penetration where they can lead to 'self-sharpening' of a projectile. In most cases, modelling adiabatic shear banding involves finite element calculations, and it is crucial to base the computations on a constitutive model adequately capturing the specifics of high speed deformation and yet simple enough as far as the number of material parameters to be identified experimentally is concerned.

A large group of empirical relations suggested to describe the variation of the flow stress with the plastic strain are generalizations of the Ludwik equation written for the case of simple shear (or torsion) as

$$\tau = A + B\gamma^n. \qquad (1)$$

Here τ and γ are the shear stress and the shear strain, respectively, and A, B and n are considered to be materials constants. To include temperature and strain rate effects, this equation was modified by several authors. Litonski (1977) suggested the form

$$\tau = C(1-aT)(1+b\dot{\gamma})^m(\gamma_o+\gamma)^n \qquad (2)$$

here T and $\dot{\gamma}$ are the absolute temperature and the shear strain rate, respectively, and C, , b, γ_o, m and n are constants. In addition to the Ludwik hardening, this form takes into account strain rate hardening and thermal softening.

olinari and Clifton (1987) and Molinari (1988) used an equation in which the effects of rain hardening, strain rate hardening and thermal softening are accounted for in a factorized power law form:

$$= \mu T^{-\nu}\dot{\gamma}^m\gamma^n \qquad (3)$$

here m, n and μ and ν are constants.

Two models which became very popular, viz. those of Johnson & Cook (1985) and rmstrong & Zerilli (1988), can also be viewed as generalizations of Ludwik's equation. owever, the strain rate dependence of the stress is taken in the logarithmic form. The Johnson-Cook equation is written as

$$= \{[1+p\ln(\dot{\gamma}/\dot{\gamma}_o)][1-T_h^{\kappa}]\}(A+B\gamma^n) \qquad (4)$$

Here $T_h = (T-T_r)/(T_m-T_r)$ is a homologous temperature, with T_m and T_r denoting the elting temperature and a reference temperature, respectively. The parameters p, $\dot{\gamma}_o$ and κ ve been introduced. The Armstrong-Zerilli model has two modifications to account for differences between bcc and fcc metals. It is interesting to note that in the fcc variant, parabolic strain hardening is coupled with a strain rate and temperature dependence. The thors should be credited for the recognition of the importance of such coupling, but the m of the constitutive equation,

$$\tau = \tau_G + B\gamma^{1/2}\exp[(-\beta_o+\beta_1\ln\dot{\varepsilon})T] + Kd^{-1/2}, \qquad (5)$$

here τ_G, β_o, β_1 and K are constants and d is the grain size, lacks a dislocation theory derpinning.

A popular model is that due to Bodner and Partom (Bodner, 1987) which is based on a ncept of an evolving internal variable that enters a kinetic equation relating the second variants of the deviatoric stress and the plastic strain rate. The form of the kinetic equation and of the evolution equation for the internal variable were chosen more or less heuristically, but with deep physical intuition. A main deficiency of the model appears to be the absence of a strain rate dependence of strain hardening (Estrin and Mecking, 1985). owever, this issue was addressed in a recent version of the model (Bodner and Rubin, 94) that does include this effect.

ability Analysis

athematical analysis of adiabatic shear banding can be demonstrated, by way of example, for the case of a thin-walled tube twisted in a torsional Kolsky bar (Costin et al., 1979). A scribe line, initially straight and parallel to the tube axis, exhibits a discontinuity when a

shear band is formed around the tube, as illustrated by Fig. 3. In this example, an adiabatic shear band in a cold rolled steel 1018 was initiated at a shear strain around 0.14 leading to fracture at a shear strain between 0.25 and 0.5 (Costin et al., 1979). The band width was in the range of 100 μm. To determine the critical conditions for the onset of strain localization, using a simple phenomenological model, Molinari (1988) carried out a linear stability analysis using a constitutive relation given by eq. (3). An idealization of the deformation geometry presented on Fig. 3 is a strip of material of height h, equal to the gauge length of the tubular specimen, deformed in simple shear in direction y (Fig. 4). The direction x is parallel to the axis of the tube and z is perpendicular to the wall. All derivatives with respect to y and z are assumed to be zero, and the deformation is zero in the direction z. The width w of the strip can be x-dependent to represent a geometrical defect. The continuum mechanics frame of the model in the simplest case when inertia is neglected is given by the compatibility condition,

$$\dot{\gamma} = \frac{\partial v}{\partial x}, \qquad (6)$$

where v is the material point velocity, and the equilibrium condition,

$$\tau w = const. \qquad (7)$$

The boundary conditions are given by v = 0 at x = 0 and v = V = $h\dot{\gamma}_{imp}$ at x = h. Here $\dot{\gamma}_{imp}$ is the nominal imposed strain rate. Assuming further that the process is adiabatic, i.e. neglecting the heat conduction and heat removal to the thermal bath, reduces the heat conduction equation to

$$Dc\dot{T} = \beta\tau\dot{\gamma} \qquad (8)$$

where D is the material density and c the specific heat capacity; the parameter β denoting the fraction of the mechanical work converted into heat is typically around 0.90-0.95. The assumption made with regard to inertia is supported by numerical simulations by Shawki (1986) who found that for steels, inertia effects *prior to onset of localization* can be neglected for nominal imposed shear rates up to 10^3 s^{-1}. Furthermore, in the pre-localization range, heat conduction does not come into play either, i.e. the adiabaticity assumption is justified as well.

Introducing a small perturbation of the (time dependent) uniform solution and identifying the onset of strain localization with the condition that this perturbation be growing with time (Clifton, 1978; Bai, 1982; Molinari, 1988), one finds easily that uniform deformation becomes unstable if

$$\frac{\beta\tau\gamma}{DcT}\cdot\frac{\nu}{n} \geq 1. \qquad (9)$$

This inequality has a very simple interpretation. In particular, it reflects the competition between the stabilizing effect of strain hardening (characterized by the parameter n) and the destabilizing effect of thermal softening (characterized by the parameter ν). It is interesting to note that in this formulation the strain rate hardening parameter m does not enter the instability condition. However, it can be shown that it determines the initial rate of growth of perturbations and does affect the kinetics of adiabatic shear banding (Molinari, 1988).

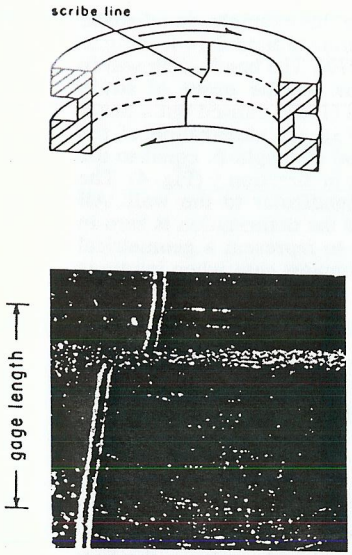

Fig. 3. Shear of a scribe line by an adiabatic shear band in a 1018 CRS steel (after Costin et al., 1979).

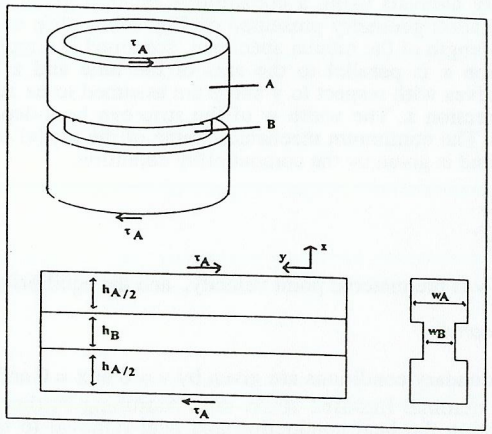

Fig. 4. Geometry of a thin-walled torsion specimen with a thickness defect as used by Costin et al. (1979) (Litonski-type specimen). Also shown is an equivalent simple shear problem for a layer infinitely extended in the y-direction.

A common - and justified - criticism of linear stability analysis concerns the fact that while the conditions for the onset of strain localization may be found adequately, the progress of localization may be slow and would not result in a macroscopic shear band (Kocks, 1985; Molinari, 1988). Full nonlinear analysis is required in order to warrant a reliable prediction. The results of such analysis will depend on the details of the constitutive model involved, as subtle features of strain hardening behaviour, and especially possible temperature and strain rate dependencies involved, will affect an interplay between stabilizing and destabilizing effects. It cannot be expected that heuristic or phenomenological models of the kind described above will capture those subtle features. Physically based models based on a detailed description of microstructure evolution during the deformation process give more promise in this regard. In the following section we shall outline one such model and shall apply it to the analysis of adiabatic shear banding in a Litonski-type specimen sketched in Fig. 3.

DISLOCATION DENSITY RELATED CONSTITUTIVE MODELLING

It is an established fact that in addition to the strain rate sensitivity of the flow stress, there is another strain rate effect that influences the deformation behaviour of metals and alloys. This dependence is associated with the rate of the microstructural evolution during the

deformation process which is reflected in the strain hardening behaviour It is commonly accepted that for a broad range of materials - and certainly for those of interest for high strain rate applications - the strain hardening coefficient decreases with strain, asymptotically tending to zero. This implies that the flow stress tends to a saturation value. Experiments show that the saturation stress is a function of strain rate and temperature and that this dependence is often stronger than the dependence on strain rate and temperature of the stress corresponding to a fixed microstructure, cf. Kocks (1976), Klepaczko and Chiem (1986), Estrin (1996). (The latter dependence can be measured in experiments in which the strain rate or temperature are changed in a jump-like manner.) The behaviour described - commonly referred to as stage III hardening - reflects a competition between athermal strain hardening and thermally activated dynamic recovery processes. Though full saturation of stress is never reached due to interference of the so-called stage IV hardening stage that sets in at very large strains, a stage III hardening model is what is needed to describe initial stages of strain localization.

Klepaczko (1975) and Kocks (1976) are to be credited for first recognizing the importance of the strain rate and temperature dependence of the strain hardening coefficient in constitutive modelling. They also put forward concepts and formulations which can be found in microstructure related constitutive models prevalent in the current literature. Their approach is based on treating the dislocation density as a microstructural internal variable and consider the dislocation density evolution as a process underlying strain hardening. A variant of a model of this type (Estrin, 1996; Molinari et al., 1995; Estrin et al, 1996) will be presented here.

The approach to dislocation density related constitutive modelling which goes back to Klepaczko and Kocks is based on the notion that the plastic strain rate is determined by glide of mobile dislocation in the material characterized by its instantaneous microstructural state. In the equation describing the glide kinetics *(the kinetic equation)* , a microstructural variable appears as a parameter. However, the microstructural state itself is considered to evolve with plastic strain. If the state is associated with the dislocation density, a description of its evolution is provided by an *evolution equation* describing the variation of the dislocation density due to dislocation storage and concurrent dislocation annihilation processes. Dislocation glide and dislocation annihilation (recovery) processes are separated in this picture. No contribution of recovery to the overall plastic strain rate is included.

A natural representation of the kinetic equation is in the Arrhenius form

$$\dot{\gamma} = \dot{\gamma}_{oo} \exp\left[-\frac{\Delta G(\tau)}{kT}\right] \tag{10}$$

where $\Delta G(\tau)$ is the stress dependent Gibbs free energy of activation for the thermally activated process of dislocation glide, k is the Boltzmann constant and $\dot{\gamma}_{oo}$ is a pre-exponential factor that for our purposes may be considered constant (Kocks et al., 1975). The structure which implicitly enters eq. (10) is specified by a single internal variable, τ_O, with which the shear stress τ scales. A convenient simplified representation of equation (10) is

$$\dot{\gamma} = \dot{\gamma}_{oo} \exp\left[-\frac{\Delta G_o}{kT}\left(1-\left(\frac{\tau}{\tau_o}\right)^p\right)^q\right] \tag{11}$$

where ΔG_0 is the value of ΔG at zero shear stress and the exponents p and q are fit parameters providing the $\dot{\gamma}$ *vs.* τ a required shape (Kocks et al., 1975; Follansbee and Kocks, 1988). An obvious deficiency of these formulas is that in the limit of $\tau \to 0$ they yield a finite plastic strain rate. However, in the present context this limit case is of no relevance.

Another representation of the kinetic equation is suggested by the fact that in analyzing thermally activated plastic deformation it is customary to present the data as $\log \dot{\gamma}$ *vs* $\log \tau$ diagrams. In what follows we adopt the power-law form of the kinetic equation:

$$\dot{\gamma} = \dot{\gamma}_o \left(\frac{\tau}{\tau_o} \right)^m . \tag{12}$$

Here the factor $\dot{\gamma}_o$ can be considered constant. This representation can only be reasonable if the power m corresponding to the slope of the $\log \dot{\gamma}$ *vs* $\log \tau$ diagram coincides with the quantity $(\partial \ln \dot{\gamma} / \partial \ln \tau)_{\tau_o}$ as obtained from the original equation (10). We thus require that

$$m = \frac{V_{act} \tau}{kT} \tag{13}$$

where $V_{act} = -\partial \Delta G(\tau) / \partial \tau$ is referred to as the activation volume of the underlying dislocation glide process. In the case under consideration, the latter quantity is given by the product of the average spacing L of localized obstacles to dislocation glide, the so called obstacle width, which quantity depends on the nature of the dislocation-obstacle interaction (and is generally shear stress dependent), and b. (A numerical constant depending on the obstacle statistics should also be included for generality.) Obviously, requiring that for a given temperature and a fixed value of τ_O both equations, (12) and (10) yield the same value of $\dot{\gamma}$ for an arbitrarily chosen τ, the pre-exponential factor $\dot{\gamma}_o$ can be expressed in terms of the quantities in equation (10). It can be estimated roughly as

$$\dot{\gamma}_o = \dot{\gamma}_{oo} \exp(-\Delta G_o / kT), \tag{14}$$

where ΔG_o is the value of the Gibbs free energy of activation ΔG at $\tau = 0$.

We focus here on face centered cubic metals where the so called Peierls stress stemming from the lattice periodicity is negligible and the obstacles to dislocation glide may be associated with impurity atoms or forest dislocations. In sufficiently pure materials the glide resistance caused by the interaction of gliding dislocations with the forest will be prevalent right from the beginning of deformation, but even with alloys, dislocation multiplication will lead the interaction with the forest to outweigh the effects due to foreign atoms as straining proceeds. In such a situation, the average obstacle spacing L proves to be governed by the average dislocation density ρ and is given by

$$L \propto 1 / \rho^{1/2} \tag{15}$$

Having in mind that the shear stress scales with $\rho^{1/2}$ (Kocks, 1976; Estrin & Mecking, 1984) and neglecting the stress dependence of the obstacle width we find that the product $V_{act} \tau$ may be considered stress independent. Introducing $A = V_{act} \tau / k$ leads to

$$m = A/T. \tag{16}$$

Measurements of the strain rate sensitivity of the flow stress in fcc metals (Duffy, 1982) confirm a reasonable constancy of A.

The situation is different with bcc materials: the activation volume for the dislocation motion in the Peierls potential can no longer be considered to be inversely proportional to the shear stress, cf. Kocks et al. (1975), and equation (16) with a constant A cannot be adopted.

In the constitutive formulation used, the structure is represented by the internal variable τ_O (referred to as the 'mechanical threshold stress' (Follansbee and Kocks, 1988)) which, in turn, is related to the dislocation density ρ (Kocks, 1987; Estrin and Mecking, 1984; Klepaczko & Chiem, 1986):

$$\tau_o = \alpha G b \rho^{1/2} \tag{17}$$

Here G is the shear modulus, b the magnitude of the dislocation Burgers vector and α is a numerical constant. An equation that represents a competition between dislocation density accumulation due to their immobilization (storage) at impenetrable obstacles and annihilation due to recovery processes,

$$d\rho / d\gamma = k_1 \rho^{1/2} - k_2 \rho \tag{18}$$

proved to be particularly adequate for describing the strain hardening behaviour in a coarse-grained single-phase material (Kocks, 1976; Estrin & Mecking, 1984). While the coefficient k_1 can be taken to be constant, the coefficient k_2 is strain rate and temperature dependent, as it reflects thermally activated recovery processes, e.g. those due to cross-slip of screw dislocations. The temperature and strain rate dependence of k_2 is expressed by

$$k_2 = k_{20} \left(\frac{\dot{\gamma}}{\dot{\gamma}_o^*} \right)^{-1/n} \tag{19}$$

Here k_{20} and $\dot{\gamma}_o^*$ are material constants, while the exponent n is temperature dependent. As discussed by Kocks (1976), this temperature dependence can be expressed by

$$n = B/T \tag{20}$$

where B is a constant for a given material. The characteristics of the material enter through the stacking fault energy χ:

$$B = \frac{Gb^3 / k}{C_1 + C_2 \chi / Gb} \tag{21}$$

Here C_1 and C_2 are constants. This phenomenological relation (Kocks, 1976) provides a description of the effect of stacking fault energy on the propensity of screw dislocations to cross-slip. A large stacking fault energy, i.e. a small B, inhibits dissociation of dislocations into partials and thus increases the probability of cross-slip.

Combining equations (12), (17), (18) and (19) leads to the following expression for the strain hardening coefficient:

$$\theta = (\partial \tau_o / \partial \gamma)_{\dot{\gamma}} = \theta_o (1 - \frac{\tau_o}{\tau_{os}}) \qquad (22)$$

where the saturation stress is given by

$$\tau_{os} = \tau^* \left(\frac{\dot{\gamma}}{\dot{\gamma}^*} \right)^{1/n} \cong \tau^* \left(\frac{\dot{\gamma}}{\dot{\gamma}_o} \right)^{1/n} \qquad (23)$$

The quantities θ_o and τ^* can be interpreted in terms of the parameters in the dislocation density evolution equation:

$$\theta_o = \alpha G b k_1 / 2; \quad \tau^* = \alpha G b k_1 / k_{20} \qquad (24)$$

Numerical calculations of the deformation behaviour for a Litonski-type specimen shown in Fig. 4 using the above constitutive model in conjunction with eqs. (6) - (8) for the constant imposed shear strain rate were carried out for OFHC copper (Estrin et al., 1996). The thickness defect was characterized by the thickness ratio, $f = w_B/w_A$, and the relative extension of the thinned portion of the specimen, $\lambda_B = h_B/(h_A+h_B)$. Here A stands for the thicker and B for the thinner part of the specimen. Representative material parameter values were chosen using the results of Tong et al. (1992), Follansbee and Kocks (1988), and Johnson (1991). Here we present some selected results of the calculations. Figure 5 shows the effect of the parameter A on the onset of strain localization. It is seen that an increasing A, i.e. a decreasing instantaneous strain rate sensitivity of the flow stress, has a destabilizing effect and leads to premature localization. The influence of the strain rate sensitivity of the strain hardening coefficient, represented by the inverse of the parameter B, is more intricate, cf. Fig. 6. It is recognized that the critical strain γ_l at which strain localization sets in depends on B in a non-monotonic way. For the values of the material and geometry parameters chosen, γ_l passes through a minimum at B = 8500 (Fig. 7). The range of B-values consistent with the material data obtained by Follansbee & Kocks (1988) corresponds to the ascending branch of the γ_l vs. B curve. At first glance, this result is hard to rationalize. Indeed, an increase of B leads to a reduction in the strain rate sensitivity of the strain hardening coefficient (and thus indirectly of stress at a given strain) and should be expected to have a destabilizing effect. However, the attendant increase of the saturation stress τ_S and of the strain hardening coefficient θ produces a concurrent stabilizing effect. It should also be noted that the attendant increase in temperature leads to a decrease of the stress exponent n and thus counteracts the increase of B. The results of numerical calculations presented in Figs. 6 and 7 suggest that the stabilizing effects prevail over the destabilizing one for B above 8500 but that the inverse is true for B below this value.

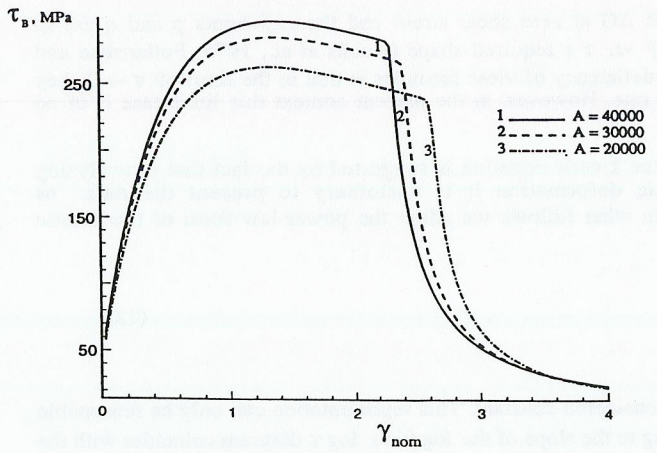

Fig. 5. The effect of the inverse instantaneous strain rate sensitivity parameter A on shear localization.

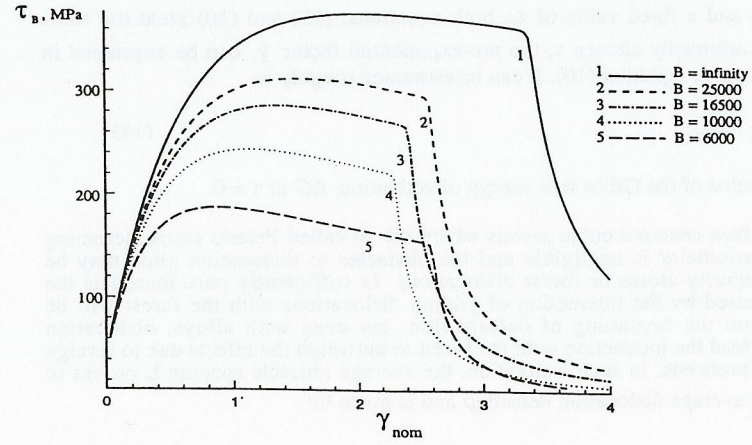

Fig. 6. The effect of the parameter B characterizing the inverse strain rate sensitivity of the strain hardening on shear localization.

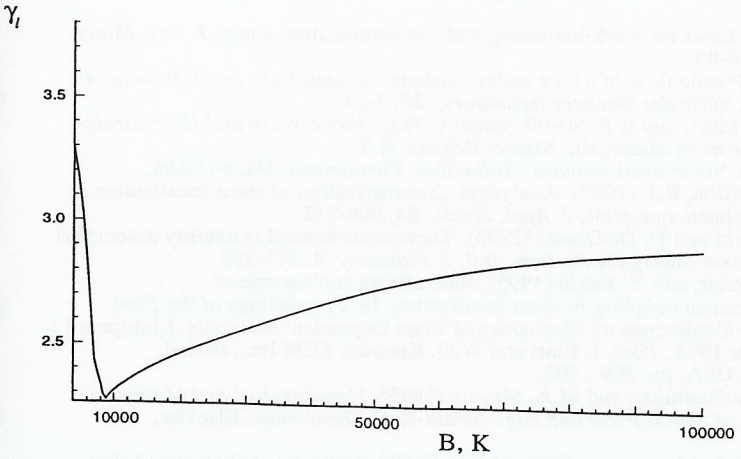

Fig. 7. Nonmonotonic dependence of the onset strain for shear localization, γ_l, on the parameter B.

The fact that for sufficiently large B the increase of this parameter leads to a delay in shear localization and also to an increase of the mechanical energy absorbed prior to shear localization can be used in alloy design. To have a localization-resistant material that possesses a large B, one can use the effect of alloying on the stacking fault energy reduction, cf. eq. (15). For example, for the case of copper, alloying with several percent Al or Si can reduce the stacking fault energy by a factor of 2-3 (Carter & Ray, 1977). This route is suitable for materials with sufficiently large B (say, larger than 8500 for the set of model parameters used in the numerical analysis of Estrin et al. (1996)). By contrast, in the opposite case of B < 8500, the recipe would be to purify the material so as to increase the stacking fault energy and decrease B, thus enhancing stability against shear localization.

The constitutive modelling frame used makes it possible to look into the effect of non-shearable second-phase particles or grain refining on adiabatic shear banding. Here we present the results for particle strengthening only. Particle effects enter through an additive, Orowan-type, contribution to the 'mechanical threshold stress':

$$\hat{\tau} = \alpha G b \rho^{1/2} + 0.84 G b / \Lambda \qquad (25)$$

where Λ is the average particle spacing in a dislocation glide plane and also through an additive storage term in the evolution equation for the dislocation density. Instead of eq. (), one has (Estrin and Mecking, 1984; Estrin, 1996)

$$d\rho / d\gamma = \beta / (b\Lambda) + k_1 \rho^{1/2} - k_2 \rho \qquad (26)$$

where β is a numerical constant, typically of the order of 0.1 to 1. The results of the calculations based on the modified equations are presented in Fig. 8. The main conclusion

is that for sufficiently small values of Λ, the critical strain for the onset of localization may decrease appreciably, while the energy absorption prior to failure is practically not affected.

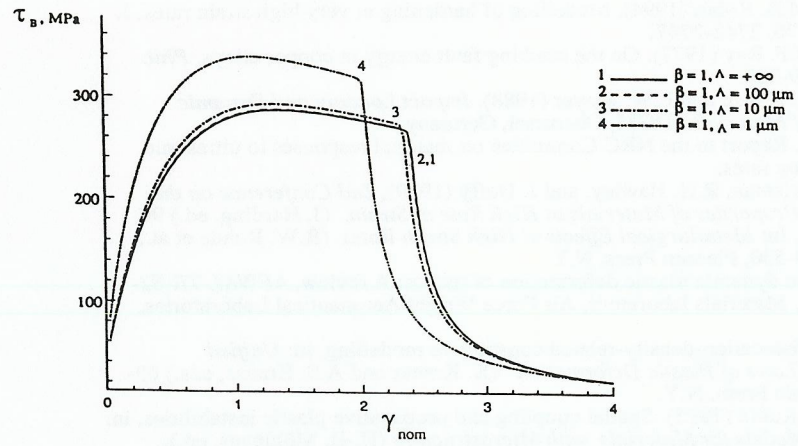

Fig. 8. The effect of second-phase particle spacing on the propensity for strain localization ($\beta = 1$).

In the cited paper (Estrin et al., 1996) it was also shown that for a model accounting for the strain rate and temperature dependence of the strain hardening in a realistic, physically relevant way, linear stability analysis fails to deliver verifiable predictions consistent with a full numerical analysis of adiabatic shear banding. Not only quantitative, but also qualitative discrepancies were found. This observation should alert researchers wishing to use linear stability analysis as a first guide to adiabatic shear localization criteria.

CONCLUSION

With this brief review we have shown that the use of microstructure-related constitutive modelling provides a possibility of consistently monitoring the effects of different metallurgical parameters, such as the solute state of an alloy or the spacing between particles of a second phase, on the resistance of the material to adiabatic shear banding. This analysis shows ways of influencing this resistance, and we see its virtue as a tool for alloy design for high strain rate applications.

ACKNOWLEDGMENTS

The authors are grateful to Sebastien Mercier for useful discussions.

REFERENCES

Armstrong, R.W., and F.J. Zerilli (1988). J. Physique, **49**, C3-529.

Bai, Y. (1982). Thermo-plastic instability in simple shear, *J. Mech. Phys. Solids* **38**, 195.

Bai, Y., and B. Dodd (1992). Adiabatic shear localization, Pergamon Press, Oxford.

Bodner, S.R. (1987). Review of a unified elastic-viscoplastic theory. In: *Unified Equations for Creep and Plasticity* (A.K. Miller, ed.), 273-301, Elsevier, London.

Bodner, S.R., and M.B. Rubin (1994), Modelling of hardening at very high strain rates, J. Appl. Phys. **76**, 2742-2747.

Carter, C.B., and I.J.F. Ray (1977). On the stacking fault energy in copper alloys, *Phil. Mag.* **35**, 189-200.

Chiem, C.-Y., H.-D. Kunze and L.W. Meyer (1988). *Impact Loading and Dynamic Behaviour of Materials* , DGM, Oberursel, Germany.

Clifton, R.J. (1978). Report to the NRC Committee on material responses to ultrasonic loading rates.

Costin, L.S., E.E. Crisman, R.H. Hawley, and J. Duffy (1979), *2nd Conference on the Mechanical Properties of Materials at High Rate of Strain,* (J. Harding, ed.) 90.

Culver, R.S. (1973). In: *Metallurgical Effects at High Strain Rates* (R.W. Rohde et al., eds.) pp. 519-530, Plenum Press, N.Y.

Duffy, J. (1982). The dynamic plastic deformation of metals: A review, *AFWAL-TR-82-4024 Report,* Materials laboratory, Air Force Wright Aeronautical Laboratories, Ohio.

Estrin, Y. (1996). Dislocation-density-related constitutive modelling, in: *Unified Constitutive Laws of Plastic Deformation* (K. Krausz and A.S. Krausz, eds.) 69-106, Academic Press, N.Y.

Estrin, Y., and L.P. Kubin (1995). Spatial coupling and propagative plastic instabilities, in: *Continuum Models for Materials with Microstructure* (H.-B. Mühlhaus, ed.), Chapter 12.

Estrin, Y., and H. Mecking (1984). A unified phenomenological description of work hardening and creep based on one-parameter models, Acta metall. **32**, 57-70.

Estrin, Y., and H. Mecking (1985). An extension of Bodner-Partom model of plastic deformation, Intl. J. Plasticity **1**, 73-85.

Estrin, Y., A. Molinari and S. Mercier (1996). The role of rate effects and of thermo-mechanical coupling in shear localisation (to be published).

Farren, W.S., and G.I. Taylor (1925). *Proc. Roy Soc. London,* **A107**, 422.

Follansbee, P.S., and U.F. Kocks (1988). A constitutive description of the deformation of copper based on the use of the mechanical threshold stress as an internal state variable, Acta metall. **36**, 81-93.

Fressengeas, C., and Molinari, A. (1987). Instability and localization of plastic flow in shear at high strain rates, *J. Mech. Phys. Solids*, **35**, 185-211.

Hartmann, K.H., H.D. Kunze, and L.W. Meyer (1981). In: *Shock Waves and High-Strain-Rate Phenomena in Metals* (M.A. Meyers and L.E. Murr, eds.) 325-327, Plenum Press.

Johnson, G.R. (1981). Dynamic analysis of a torsion test specimen including heat conduction and plastic flow", *ASME J. Eng. Mater. Techn.* **103**, 201-206.

Johnson, G.R., and W.H. Cook (1985). *Eng. Fract. Mech.* **21**, 31.

Klepaczko, J. (1975). Thermally activated flow and strain rate history effects for some polycrystalline f.c.c. metals, *Mater. Sci. Eng.* **18**, 121-135.

Klepaczko, J.R., and Chiem, C.Y. (1986). On rate sensitivity of f.c.c. metals, instantaneous rate sensitivity and rate sensitivity of strain hardening, *J. Mech. Phys. Solids*, **34**, 29-54.

Kocks, U.F. (1981). *Progr. Mater. Sci.,* **19**, 125.

Kocks, U.F., A.S. Argon, and M.F. Ashby (1975). Thermodynamics and kinetics of slip, Pergamon Press., Oxford.

Kocks, U.F. (1976). Laws for work-hardening and low-temperature creep. *J. Eng. Mater. Techn.* **98**, 76-85.

Litonski, J. (1977). Plastic flow of a tube under adiabatic torsion, *Bull. Acad. Polonaise des Sciences, Série des Sciences techniques,* **25**, 7-14.

Meyers, M.A., L.E. Murr, and K.P. Staudhammer (1992). *Shock-Wave and High-Strain-Rate Phenomena in Materials,* Marcel Dekker, N.Y.

Molinari., A. (1988). Shear band analysis, *Solid State Phenomena*, **3/4**, 447-468.

Molinari, A., and Clifton, R.J. (1987). Analytical characterization of shear localization in thermoviscoplastic materials, *J. Appl. Mech.* **54,** 806-812.

Molinari, A., Y. Estrin and D. Dudzinski (1993). Thermomechanical instability associated with heat release during plastic flow, *Intl. J. Plasticity* **9**, 317-333.

Molinari, A., S. Mercier, and Y. Estrin (1995). Rate effects and the role of thermomechanical coupling in shear localization. In: Proceedings of the First International Conference on Mechanics of Time Dependent Materials, Ljubljana 11-13 September 1995, (Eds. I. Emri and W.G. Knauss), SEM Inc., Bethel, Connecticut, USA, pp. 299 - 303.

Murr, L.E., K.P. Staudhammer, and M.A. Meyers (1995). *Metallurgical and Materials Applications of Shock-Wave and High-Strain-Rate Phenomena*, Elsevier, Amsterdam.

Nesterenko, V.F., M.A. Meyers, and T.W. Wright (1995). Collective behaviour of shear bands, in Murr et al., 1995.

Stepanov, A.W. (1933), *Phys. Z. Sowjetunion* **4**, 609.

Tong, W., Clifton, R.J, and Huang, S. (1992). Pressure-shear impact investigation of strain rate history effects in oxygen-free high-conductivity copper", *J. Mech. Phys.Solids* **40**, 1251-1294.